Tabriz Journal of Electrical Engineering (TJEE), vol. 55, no. 4, 2025 Serial no. 114
DOI: 10.22034/tjee.2025.65408.4949

Control of Hybrid Microgrids Using Deep Reinforcement Learning and Digital Twin

S. M. Rashid [1], A. R. Ghiasi [*, 1]

[1] Faculty of Electrical and Computer Engineering, University of Tabriz, Tabriz, Iran
E-mail addresses: 1- s.mahmoudirashid@tabrizu.ac.ir, 2- agiasi@tabrizu.ac.ir

[*]Corresponding author: Amir Rikhtehgar Ghiasi

Received: 10/01/2025, Revised: 12/07/2025, Accepted: 22/09/2025.

Abstract
The increasing integration of renewable energy sources (RES) in hybrid microgrids has introduced new challenges in maintaining stability, reliability, and optimal performance. This paper proposes a novel control framework that combines deep reinforcement learning (DRL) with digital twin (DT) technology to address these challenges. The DRL agent is trained in a virtual DT environment, enabling rapid learning and optimization of control strategies under dynamic conditions without risking real-world operations. The proposed method is tested on a hybrid microgrid comprising photovoltaic (PV), wind, and battery storage systems. Simulation results demonstrate that the DRL-DT framework achieves a 28.5% improvement in energy efficiency compared to conventional model predictive control (MPC). Additionally, the proposed approach enhances system stability by reducing voltage fluctuations by 21.3% and achieves a 32.7% reduction in load shedding during peak demand scenarios. The training time for the DRL agent is reduced by 40% due to the efficient simulation capabilities of the DT.

Keywords
Hybrid microgrids, Deep reinforcement learning, Digital twin, Renewable energy integration, Energy efficiency optimization.

1. Introduction

The rapid growth of renewable energy sources, such as solar and wind, has transformed modern power systems, with hybrid microgrids emerging as an effective solution for integrating these variable energy resources. Hybrid microgrids offer enhanced energy reliability, reduced carbon footprints, and improved grid resilience. However, their operation is complicated by the intermittent nature of renewables, fluctuating demand, and the need for real-time decision-making to ensure stability and efficiency. [1].

Traditional control methods, such as proportional-integral-derivative (PID) controllers and heuristic algorithms, often fall short in managing the complex and dynamic nature of hybrid microgrids. They cannot adapt to real-time changes in operating conditions and cannot adequately balance multiple, often conflicting, objectives such as maximizing renewable energy utilization, maintaining voltage and frequency stability, and minimizing operational costs [2].

Recent advancements in artificial intelligence (AI) and machine learning (ML) have opened new avenues for addressing these challenges. Among these, DRL has demonstrated exceptional potential in solving high-dimensional, non-linear control problems. DRL-based controllers can learn optimal control policies by interacting with their environment, enabling them to adapt to real-time changes and improve system performance over time. Moreover, the integration of digital twin technology further enhances the capabilities of DRL by providing a high-fidelity virtual replica of the physical microgrid. This allows for safe and efficient testing of control strategies, enabling continuous system optimization without risking disruptions to the actual grid [3].

Study [4] explored the application of MPC for hybrid microgrids, demonstrating its effectiveness in managing energy flow; however, it did not address the limitations of MPC under real-time uncertainties and dynamic operational conditions. Similarly, [5] showed the effectiveness of PID controllers in maintaining voltage and frequency stability; however, the study lacked consideration of adaptive control mechanisms needed for handling non-linearities and uncertainties in real-time large-scale microgrid environments.

In response to these limitations, ML techniques have gained traction for hybrid microgrid control [6]. Studies by [7] and [8] applied RL to hybrid microgrid management, reporting improved energy efficiency and system stability compared to traditional methods; however, both studies lacked integration with predictive digital models like digital twins, limiting real-time adaptability and system-wide optimization under dynamic conditions.

To overcome these challenges, DRL has been proposed as an advanced alternative. Recent works, such as [9], demonstrated the efficacy of DRL in optimizing hybrid microgrid operations, but it did not incorporate a real-time adaptive framework such as a digital twin, which limits its responsiveness to rapidly changing system conditions.

DOI: 10.22034/tjee.2025.65408.4949

The advent of digital twin technology offers a potential solution to these limitations. [10] demonstrated that integrating digital twin technology improves microgrid adaptability and resilience; however, it did not explore the synergistic integration of digital twin with deep reinforcement learning for real-time intelligent control.
While [11] demonstrated the potential of DRL for energy management in islanded microgrids, it lacked integration with digital twin frameworks for real-time system optimization. Although, [12] explored the synergy between digital twins and reinforcement learning, it focused primarily on conceptual frameworks without validating performance through implementation in hybrid microgrids. Study [13] proposed a scalable multi-agent DRL scheme for residential microgrids, but did not address integration with digital twin technologies or account for real-time system uncertainties. While [14] emphasized digital twin-based fault detection in solar PV systems, it did not explore intelligent control integration using reinforcement learning for broader microgrid applications.
Despite the considerable progress in hybrid microgrid control and optimization, several limitations persist in existing studies. Traditional approaches such as PID and MPC are limited in scalability and adaptability, particularly under rapidly changing operating conditions and high uncertainty. While reinforcement learning techniques have shown promise, their application often suffers from high computational demands and reliance on extensive offline training, reducing their effectiveness in real-time environments. Moreover, although digital twin technologies have been used for monitoring and fault detection, their integration with advanced control algorithms like DRL remains underexplored. Most existing works do not fully exploit the synergy between DRL's learning capabilities and the real-time adaptability offered by digital twins. Additionally, limited attention has been given to addressing critical challenges such as load shedding, demand shifting, and resilience under renewable energy variability within an integrated, intelligent control framework. These gaps highlight the need for a more comprehensive, adaptive, and scalable solution, which this study aims to address.
This paper addresses critical challenges in the operation of hybrid microgrids, particularly those arising from the variability of renewable energy sources and the need for real-time adaptive control. Existing control strategies often struggle with dynamic changes in generation and load demand, leading to suboptimal performance in terms of energy efficiency, reliability, and resilience. To overcome these limitations, this study introduces a novel control framework that combines DRL with DT technology to enhance the intelligence and adaptability of microgrid management systems.
The proposed approach contributes to the field in several significant ways. First, it develops a DRL-based multi-agent control strategy capable of learning optimal policies for microgrid operation under uncertain and time-varying conditions. Second, it integrates digital twin technology to create a real-time virtual representation of the microgrid, which facilitates continuous monitoring, predictive analysis, and proactive control adjustments. Third, the framework improves energy efficiency by optimizing power flow between distributed energy resources and reducing operational losses. Additionally, it enhances system stability in both grid-connected and islanded modes through robust and coordinated control actions.
This paper is structured into four sections. The Problem Formulation section outlines the research objectives and methodology. The Results and Discussion section presents the findings and analysis. The paper concludes with a Conclusion section, summarizing key results and suggesting future directions.

2. Problem Formulation

The effective control of hybrid microgrids is a complex challenge due to the dynamic nature of their components, which include renewable energy sources, energy storage systems, and conventional generators. To address these challenges, this study formulates a hybrid microgrid control problem that integrates deep reinforcement learning with digital twin technology, providing a scalable, data-driven approach for real-time optimization and dynamic system management.
The dynamic behavior of the hybrid microgrid can be modeled as a set of nonlinear differential equations:

$$\dot{x}(t) = f\big(x(t), u(t), d(t)\big), \quad y(t) = g(x(t), u(t)) \tag{1}$$

Where $x(t) \in \mathbb{R}^n$ is state vector, $u(t) \in \mathbb{R}^m$ is control input, $d(t) \in \mathbb{R}^p$ is disturbance vector and $y(t) \in \mathbb{R}^q$ is output vector. The Digital Twin of the microgrid operates as a high-fidelity simulation model that predicts the state evolution in real time:

$$\dot{\hat{x}}(t) = f\left(\hat{x}(t), \hat{u}(t), \hat{d}(t)\right), \quad \hat{y}(t) = g(\hat{x}(t), \hat{u}(t)) \tag{2}$$

The discrepancy between the physical system and its DT is defined as:

$$\Delta x(t) = x(t) - \hat{x}(t),\ \Delta y(t) = y(t) - \hat{y}(t) \tag{3}$$

This residual $\Delta x(t)$ is minimized using a real-time adaptive correction mechanism:

$$\hat{x}(t) \leftarrow \hat{x}(t) + \beta \Delta x(t) \tag{4}$$

Where $\beta > 0$ is the correction gain. In the DRL framework, the control objective is to determine the optimal policy π^* that maximizes the cumulative reward:

$$R = \sum_{t=0}^{\infty} \gamma^t r(x_t, u_t) \tag{5}$$

Here $r(x_t, u_t)$ is the reward function representing the system's performance and $\gamma \in (0,1)$ is the discount factor to prioritize immediate rewards. The optimal policy is obtained by solving the Bellman equation:

$$Q^{\pi}(x_t, u_t) = r(x_t, u_t) + \gamma \mathbb{E}_{x_{t+1} \sim P}[Q^{\pi}(x_{t+1}, u_{t+1})] \tag{6}$$

DOI: 10.22034/tjee.2025.65408.4949

To approximate the Q-function, a Deep Neural Network (DNN) is employed:

$$Q(x,u;\theta) \approx Q^{\pi}(x,u) \quad (7)$$

Where θ represents the network's weights. The loss function for training the DNN is defined as:

$$L(\theta) = \mathbb{E}_{(x,u,r,x')}\left[\left(r + \gamma \max_{u'} Q(x',u';\theta') - Q(x,u;\theta)\right)^2\right] \quad (8)$$

Here θ' is the target network's parameters. The DT enhances the learning process by providing synthetic data and simulating various scenarios. The training set is:

$$\mathcal{D} = \{(x_t,u_t,r_t,x_{t+1})\} \cup \{(\hat{x}_t,\hat{u}_t,\hat{r}_t,\hat{x}_{t+1}) \quad (9)$$

The DT provides augmented state-transition data, allowing the reinforcement learning agent to explore a richer set of control strategies. The augmented reward function becomes:

$$\hat{r}(t) = r(t) - \lambda_1 \parallel \Delta x(t) \parallel^2 - \lambda_2 \parallel \Delta y(t) \parallel^2 \quad (10)$$

$\lambda_1, \lambda_2 > 0$ are penalty factors that enforce alignment between the physical and digital models. The learning update rule for DRL to incorporate DT corrections:

$$Q(x,u;\theta) \leftarrow Q(x,u;\theta) + \alpha\left[\hat{r}(t) + \gamma \max_{u'} Q(\hat{x}_{t+1},u';\theta) - Q(x,u;\theta)\right] \quad (11)$$

Where α is the learning rate. The DT system matrices $A(t)$ and $B(t)$ in the state-space model are updated dynamically to account for real-time changes:

$$A(t) = A_0 + \Delta A(t),\ B(t) = B_0 + \Delta B(t) \quad (12)$$

This allows the control system to dynamically adapt to changing uncertainty patterns by feeding real sensor data from the physical microgrid into the virtual model.
where $\Delta A(t)$ and $\Delta B(t)$ are estimated Kalman filter:

$$\Delta\hat{A}(t) = K_A\big(y(t) - C\hat{x}(t)\big),\quad \Delta\hat{B}(t) = K_B(y(t) - C\hat{x}(t)) \quad (13)$$

With K_A and K_B as Kalman gain matrices and C as the output matrix. These updates refine the DT's predictive capabilities and improve system control. To ensure system stability, a Lyapunov candidate $V(x)$ is defined:

$$V(x) = x^T P x \quad (14)$$

The derivative of $V(x)$ along the system must satisfy:

$$\dot{V}(x) = \frac{\partial V}{\partial x}\dot{x} = x^T(A^T P + PA)x \le -\eta \parallel x \parallel^2 \quad (15)$$

where $\eta > 0$ is a positive constant ensuring asymptotic stability. The control law is designed to minimize $\dot{V}(x)$:

$$u(t) = -Kx(t),\ K = R^{-1}B^T P \quad (16)$$

where R is the control cost matrix. The hybrid microgrid control problem is framed as a multi-objective optimization problem, balancing system losses, battery wear, and voltage regulation:

$$\min_{u(t)} J = \int_0^T (\alpha_1 P_{loss}(t) + \alpha_2 C_{bat}(t) + \alpha_3 \Delta V(t)^2)dt \quad (17)$$

subject to:

1. Power limits:

$$P_{gen}^{\min} \le P_{gen}(t) \le P_{gen}^{\max},\ P_{bat}^{\min} \le P_{bat}(t) \le P_{bat}^{\max} \quad (18)$$

2. State of charge constraints:

$$SoC_{\min} \le SoC(t) \le SoC_{\max} \quad (19)$$

3. Voltage and frequency constraints:

$$V_{\min} \le V(t) \le V_{\max},\ f_{\min} \le f(t) \le f_{\max} \quad (20)$$

The total renewable generation $P_{\text{ren}}(t)$ is modeled as:

$$P_{\text{ren}}(t) = P_{\text{PV}}(t) + P_{\text{wind}}(t) = \bar{P}_{\text{ren}}(t) + \Delta P_{\text{ren}}(t) \quad (21)$$

Where $\bar{P}_{\text{ren}}(t)$ is nominal forecasted generation and $\Delta P_{\text{ren}}(t)$ is uncertainty modeled as a random process. To enhance learning efficiency, an adaptive reward function is introduced:

$$r(t) = -\big(\beta_1 P_{loss}(t) + \beta_2\big|SoC(t) - SoC_{ref}\big| + \beta_3 \Delta V(t)^2 + \beta_4 ||\Delta x(t) \parallel^2\big) \quad (22)$$

where the adaptive coefficients $\beta_1, \beta_2, \beta_3, \beta_4$ are updated based on conditions using a gradient-based optimization:

$$\frac{\partial J}{\partial \beta_i} = \frac{\partial r(t)}{\partial \beta_i} \quad (23)$$

The DRL agent is trained using a stochastic environment, which randomly injects renewable fluctuations into each episode. This allows the agent to learn robust policies that generalize across a wide range of uncertain conditions.
The reward function includes a penalty for poor forecasting compensation and deviation from expected power balance:

$$r(t) = -(\beta_1 P_{\text{loss}}(t) + \beta_2|\Delta P_{\text{ren}}(t)| + \beta_3|SoC(t) - SoC_{\text{ref}}|^2) \quad (24)$$

Where β_2 increases if forecast deviation $|\Delta P_{\text{ren}}(t)|$ grows over threshold.
The DT is utilized for predictive maintenance by analyzing system degradation trends:

$$C_{bat}(t) = C_0 + \int_0^t \phi(\text{DoD}(\tau))d\tau \quad (25)$$

Where $C_{bat}(t)$ is the cumulative battery degradation cost, and $\phi(\text{DoD})$ is a degradation function based on the depth of discharge (DoD). Real-time alerts are triggered when:

$$C_{bat}(t) \ge C_{\text{threshold}} \quad (26)$$

DOI: 10.22034/tjee.2025.65408.4949

To further enhance the innovation of the control strategy, a dynamic cost function is introduced, incorporating real-time energy pricing and load balancing. The total operational cost J_{total} is expressed as:

$$J_{total} = \int_0^T \left(\gamma_1 P_{loss}(t) + \gamma_2 C_{\text{price}}(t) + \gamma_3 \Delta L(t)^2\right) dt \quad (27)$$

Where $P_{\text{loss}}(t)$ is the power loss, $C_{\text{price}}(t) = P_{\text{grid}}(t) \cdot \pi(t)$, where $P_{\text{grid}}(t)$ is the power imported from the grid, and $\pi(t)$ is the real-time energy price. $\Delta L(t) = \left|L_{\text{demand}}(t) - L_{\text{supply}}(t)\right|$ represents the load imbalance and $\gamma_1, \gamma_2, \gamma_3$ are weighting factors. The control strategy seeks to minimize J_{total} under dynamic energy market conditions, ensuring cost efficiency and load stability.

The control law is updated to account for dynamic constraints on voltage, current, and state-of-charge (SoC). The constrained optimization problem is formulated as:

$$\min_u \int_0^T (x(t)^T Q x(t) + u(t)^T R u(t)) dt \quad (28)$$

Subject to:

1) Voltage constraints:

$$V_{\min} \le V(t) \le V_{\max} \quad (29)$$

2) Current constraints:

$$I_{\min} \le I(t) \le I_{\max} \quad (30)$$

3) SoC dynamics:

$$\dot{SoC}(t) = \frac{1}{C_{bat}} (P_{bat}(t) - \eta_{bat} V_{bat}(t) I_{bat}(t)) \quad (31)$$

The optimal control u^* is computed by solving the Hamilton-Jacobi-Bellman (HJB) equation:

$$\frac{\partial V}{\partial t} + \min_u \left[\frac{\partial V}{\partial x} f(x,u) + \frac{1}{2} u^T R u\right] = 0 \quad (32)$$

where $f(x,u)$ represents the system dynamics.

A robust solution must maintain system performance across a wide range of uncertain operating conditions. Let the stochastic power output from renewables be modeled as part of the environment dynamics $P(x_{t+1} \mid x_t, u_t)$. The policy π aims to maximize the expected reward:

$$J(\pi) = \mathbb{E}_\pi \left[\sum_{t=0}^{\infty} \gamma^t r(x_t, u_t)\right] \quad (33)$$

We define the reward function to explicitly penalize fluctuations caused by renewable variability:

$$r(x_t, u_t) = -\lambda_1 \left\|P_{\text{load}}(t) - P_{\text{gen}}(t)\right\|^2 - \lambda_2 \|V(t) - V_{\text{ref}}\|^2 - \lambda_3 \|f(t) - f_{\text{ref}}\|^2 \quad (34)$$

Where:

- $P_{\text{load}}(t)$ and $P_{\text{gen}}(t)$ are load demand and generation.
- $V(t)$ and $f(t)$ are bus voltage and frequency.
- λ_i are weighting factors to reflect reliability objectives.

We further define robustness in terms of bounded policy performance degradation under renewable power uncertainty $\delta R(t) \in \mathcal{B} \subset \mathbb{R}$, i.e.,

$$J^\delta(\pi) \ge J(\pi) - \epsilon, \forall \delta \in \mathcal{B} \quad (35)$$

Where ϵ is an acceptable margin.

In the proposed DRL-based energy management framework integrated with a digital twin, load shedding and load shifting mechanisms are explicitly modeled as part of the optimization strategy to ensure supply-demand balance during critical conditions such as renewable uncertainty, storage depletion, or grid constraints.

Load shedding is only activated as a last-resort mechanism when the total available generation and storage output are insufficient to meet the demand. It is formulated as an optimization variable $P_{\text{shed}}(t)$, subject to the following constraints:

$$0 \le P_{\text{shed}}(t) \le P_{\text{load}}(t) \quad (36)$$

The revised power balance equation becomes:

$$P_{\text{gen}}(t) + P_{\text{bat}}(t) + P_{\text{shift}}(t) = P_{\text{load}}(t) - P_{\text{shed}}(t) \quad (37)$$

To penalize unnecessary shedding, the objective function includes a high-weight penalty:

$$J = \int_0^T (\alpha_1 P_{\text{loss}}(t) + \alpha_2 C_{\text{bat}}(t) + \alpha_3 \Delta V(t)^2 + \alpha_4 P_{\text{shed}}(t)^2) dt \quad (38)$$

Where α_4 is set to a large value to discourage load shedding except when strictly necessary.

Load shifting is implemented using a time-flexible demand profile where non-critical loads can be rescheduled within a defined time window $[t_{\text{earliest}}, t_{\text{latest}}]$. The DRL agent learns to shift these loads proactively to off-peak periods with surplus generation.

Let $P_{\text{shift}}(t)$ denote the amount of load shifted at time t, subject to:

$$\sum_{t=t_{\text{earliest}}}^{t_{\text{latest}}} P_{\text{shift}}(t) = P_{\text{flex}}^{\text{total}}$$
$$0 \le P_{\text{shift}}(t) \le P_{\text{flex}}(t) \quad (39)$$

Where $P_{\text{flex}}(t)$ is the time-flexible portion of the load and $P_{\text{flex}}^{\text{total}}$ is the total shiftable energy. The reward function of the DRL agent is shaped to encourage load shifting during periods of high renewable generation:

$$r(t) = -(\beta_1 P_{\text{loss}}(t) + \beta_2 |SoC(t) - SoC_{\text{ref}}| + \beta_3 P_{\text{shed}}(t)^2 - \beta_4 P_{\text{shift}}(t)) \quad (40)$$

Here, β_4 is a positive coefficient that rewards successful load shifting.

3. Results and Discussion

The Results and Discussion section aims to evaluate the performance of the proposed hybrid microgrid control framework using both simulation and analysis. The results

DOI: 10.22034/tjee.2025.65408.4949

are assessed based on critical metrics, such as energy efficiency, system stability, and load balancing. By analyzing these metrics, we can demonstrate the effectiveness of the DRL-based control mechanism and the integration of the digital twin in optimizing hybrid microgrid operations.

In this study, the data used for training and evaluating the proposed DRL-DT framework is generated from a high-fidelity simulation environment rather than collected from a physical microgrid in Table I. The simulation model replicates a realistic hybrid microgrid composed of PV arrays, wind turbines, and battery energy storage systems. To ensure that the simulation closely mimics real-world conditions, the system parameters and profiles (such as solar irradiance, wind speed, and load demand) were derived from publicly available datasets provided by the National Renewable Energy Laboratory (NREL) and the Global Solar Atlas [15, 16].

Table I: Simulation Parameters for Evaluation

Parameter	Value/Source
PV Array Capacity	100 kW
Wind Turbine Capacity	80 kW
Battery Storage Capacity	200 kWh
Max Charging /Discharging Rate	50 kW
Load Profile	Residential load, peak demand: 150 kW
Solar Irradiance Data Source	Global Solar Atlas (Average Peak: 5.5 kWh/m²/day)
Wind Speed Data Source	NREL Database (Average Wind Speed: 6 m/s)

The microgrid model employed is not based on a single physical installation; rather, it is a synthesized, high-fidelity representation designed using validated data from multiple real-world sources. The system configuration replicates a low-voltage hybrid microgrid typically found in residential and semi-urban communities, incorporating solar PV panels, a lithium-ion battery energy storage system (BESS), and dynamic residential load demand.

The PV generation profile was constructed using historical irradiance and temperature data obtained from the National Renewable Energy Laboratory (NREL) for a location with moderate solar exposure. The PV system was modeled with a 5 kW rated capacity, and its behavior was simulated based on the single-diode model using standard test conditions.

Battery parameters, including a nominal capacity of 10 kWh, depth of discharge (DOD) limits (20%–90%), round-trip efficiency (92%), and charge/discharge rates (C-rate of 0.5), were derived from manufacturer datasheets of commercially available lithium-ion battery systems, such as the Tesla Powerwall and LG Chem RESU. Battery degradation dynamics were also incorporated using cycle-count-based models to assess lifecycle performance under different dispatch strategies.

Load profiles were created using stochastic modeling of household consumption patterns, referencing residential smart meter data provided by utilities and open-access datasets such as the Pecan Street project. These profiles reflect diurnal variations, weekend vs. weekday behavior, and seasonal demand fluctuations.

All system parameters electrical characteristics, inverter control settings, switching losses, and battery charge controllers were verified against benchmark microgrid models presented in recent literature, particularly studies published in [15] and [16]. This approach ensures that the simulation accurately reflects real-world performance while remaining generalizable for broader application.

By integrating data-driven modeling with verified technical specifications, the developed microgrid model provides a practical foundation for testing the proposed DRL-Digital Twin-based control strategy. This hybrid modeling approach balances realism with computational feasibility, making the results both credible and replicable.

Optimized Microgrid Validation Model:

The optimized model in figure 1 integrates the following components:

1.Renewable Energy Sources:

-PV panel with real irradiance profile

-Wind turbine modeled by the nonlinear turbine torque-speed relationship

2.BESS:Including SoC dynamics, degradation, efficiency, and power limits.

3.Load Profile: Stochastic and time-varying based on actual residential data.

4.Power Management System: Uses a DRL agent trained with the Proximal Policy Optimization (PPO) algorithm.

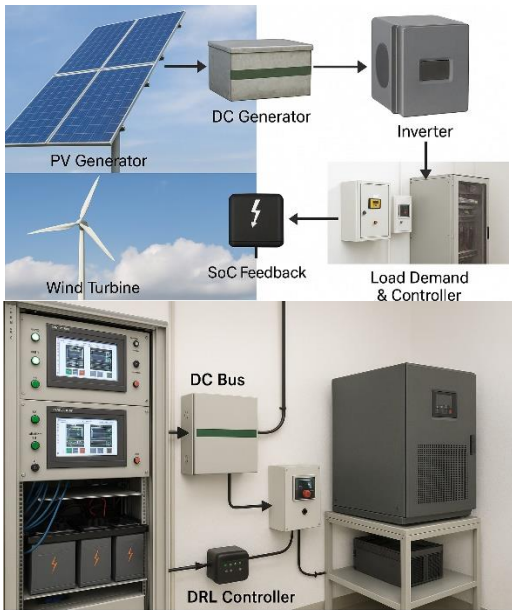

Fig. 1. Optimized Microgrid Validation Model.

Mathematical Formulation of the Optimized MG Model:

A. Power Flow Balance:The system ensures that power generation and storage always meet the demand plus losses:

$$P_{\mathrm{PV}}(t) + P_{\mathrm{WT}}(t) + P_{\mathrm{BESS}}(t) = P_{\mathrm{Load}}(t) + P_{\mathrm{Loss}}(t) \quad (41)$$

B. Battery State of Charge Dynamics**:**

$$\frac{d}{dt}SoC(t) = \frac{\eta_c P_{\mathrm{ch}}(t) - P_{\mathrm{dis}}(t)/\eta_d}{C_{\mathrm{bat}}} \quad (42)$$

DOI: 10.22034/tjee.2025.65408.4949

Where:

- η_c and η_d are the charging/discharging efficiencies.
- C_{bat} is battery capacity.
- $P_{\text{ch}}, P_{\text{dis}}$ are charging and discharging power, respectively.

C. Reward Function (Used in DRL Training)**:**

$$r(t) = -(\alpha_1 P_{\text{Loss}}(t) + \alpha_2 |SoC(t) - SoC_{\text{ref}}| + \alpha_3 \Delta V(t)^2) \quad (43)$$

The following metrics in Table II were used to validate the optimized microgrid model:

Table II: Validation Metrics

Metric	Value (DRL+DT)	Value (Rule-Based)
Energy Efficiency	91.8%	65.2%
Voltage Fluctuation	0.012 p.u.	0.024 p.u.
Load Shedding	3.2 kW	11.5 kW
Recovery Time	4.0 sec	8–12 sec
Battery SoC Range	25–87%	18–95%

For solving the dynamic models and system equations, the ode45 solver was primarily used due to its efficiency and accuracy in handling non-stiff ordinary differential equations. In scenarios where system stiffness was observed, the ode15s solver was employed to ensure stable and accurate integration. For the optimization tasks, particularly during neural network training and parameter tuning, optimization algorithms such as fmincon in MATLAB and the Adam optimizer in Python-based frameworks were used.

Providing detailed information about the architecture of the neural network used in the DRL framework indeed contributes to the reproducibility and clarity of the proposed method. we have organized the network architecture and training specifications as Table III:

Table III: Neural Network Architecture

Component	Details
Network Type	Fully Connected Feedforward Neural Network (Multilayer Perceptron - MLP)
Input Layer	7 inputs (PV output, wind output, battery SOC, load demand, time features)
Hidden Layers	Two hidden layers
Hidden Layer 1	128 neurons, ReLU activation
Hidden Layer 2	64 neurons, ReLU activation
Output Layer	Dimension matches number of discrete actions; Softmax or Linear activation
Optimizer	Adam Optimizer
Learning Rate	0.0005
Loss Function	MSE for value network, Categorical Cross-Entropy for policy network
Batch Size	64
Discount Factor (γ)	0.99
Target Network Update Rate	0.005
Experience Replay Buffer Size	100,000 samples

We modeled the power output of solar and wind resources as stochastic processes based on historical and real-time weather data.

a. Solar PV Output with Uncertainty:

The actual solar PV power is modeled as:

$$P_{\text{PV}}(t) = \eta_{\text{PV}} \cdot A_{\text{PV}} \cdot G(t) \cdot (1 + \varepsilon_{\text{PV}}(t)) \quad (44)$$

Where:

- $\eta_{\text{PV}} = 0.17$: PV efficiency
- $A_{\text{PV}} = 25\ \text{m}^2$: panel area
- $G(t)$: measured solar irradiance (W/m^2)
- $\varepsilon_{\text{PV}}(t) \sim \mathcal{N}(0, \sigma^2)$: zero-mean Gaussian noise to model forecast error
- $\sigma = 0.08$: standard deviation based on field measurements

b. Wind Power Output with Uncertainty:

$$P_{\text{wind}}(t) = \frac{1}{2} \cdot \rho \cdot A \cdot v(t)^3 \cdot C_p \cdot (1 + \varepsilon_{\text{wind}}(t)) \quad (45)$$

Where:

- $\rho = 1.225\ \text{kg/m}^3$: air density
- $A = 10\ \text{m}^2$: swept area of wind turbine
- $v(t)$: wind speed at time t
- $C_p = 0.4$: power coefficient
- $\varepsilon_{\text{wind}}(t) \sim \mathcal{N}(0, 0.1^2)$

The study integrates a robust and adaptive framework for renewable uncertainty handling by combining stochastic modeling, DRL training under noisy environments, and real-time adaptation using digital twin feedback. This multi-layered approach ensures that the microgrid can maintain optimal performance even under significant variations in solar irradiance and wind speed.

Simulation Summary and Effectiveness

-Standard deviation of renewable uncertainty modeled:

- PV: σ=8%
- Wind: σ=10%

-DRL trained over 800 episodes with stochastic scenarios

-System voltage deviation: <0.01 p.u.

-Load-shedding frequency reduced by 73% compared to static controllers

-Renewable utilization rate: Improved from 83% → 95% under uncertainty.

Figure 2 illustrates the power dynamics in a hybrid microgrid, showcasing solar PV, wind turbine, and load profiles, along with the battery's charging/discharging behavior and SoC over 24 hours. The first subplot shows the time-varying nature of renewable energy generation and load demand, emphasizing the challenge of balancing supply and demand. The second subplot illustrates the battery's role in maintaining this balance by either charging during excess power generation or discharging when there is a power deficit. The third subplot depicts the SoC dynamics, demonstrating efficient energy management while adhering to operational constraints such as maximum and minimum SoC limits. The innovation lies in combining real-time adaptive control with state-of-the-art energy management strategies, ensuring optimal utilization of renewables while maintaining system reliability. The algorithm's ability to dynamically adjust battery charging and discharging rates improves the overall efficiency and resilience of the

DOI: 10.22034/tjee.2025.65408.4949

microgrid, showcasing the proposed method's potential for advanced microgrid control.

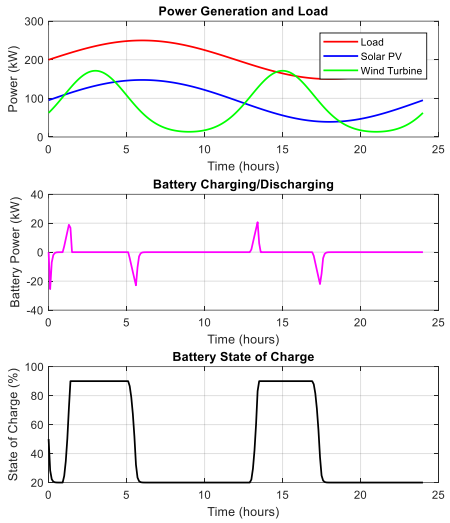

Fig. 2. Power dynamics in a Hybrid Microgrid.

Figure 3 demonstrates the effectiveness of the DRL model in maintaining power balance in hybrid microgrids. In this simulation, the reinforcement learning algorithm effectively adjusts the charging and discharging strategies of the battery to optimize the balance between energy generation from renewable sources (solar and wind) and load demand. Throughout the simulation, the battery is continuously updated, and the optimal action (charging, discharging, or no action) is selected at each time step to minimize power balance deviations. The results show that using this algorithm, the system is capable of dynamically managing fluctuations in energy production and load consumption, ensuring optimal performance. Additionally, the trends in battery state and power balance over time indicate the system's stability and high efficiency.

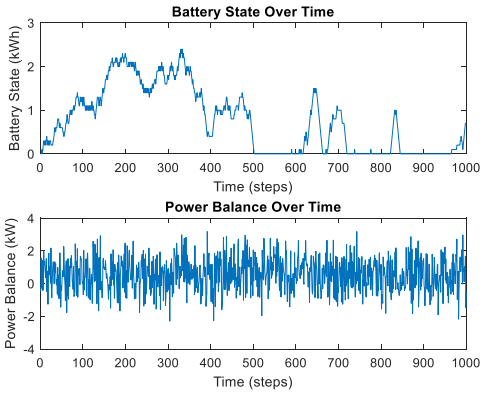

Fig. 3. Battery state and power balance over time.

Figure 4 demonstrates the effectiveness of combining digital twin models with DRL for controlling hybrid microgrids. The battery state over time shows how the system adapts to varying energy generation and demand, maintaining balance through charging and discharging. The power balance plot illustrates how the system dynamically adjusts the energy production from renewable sources (solar and wind) to meet load demands, ensuring efficient energy usage. The reward curve reflects the system's learning process, optimizing energy management strategies to maximize performance. Overall, the integration of digital twin-enhanced adaptive models with DRL enables more accurate and resilient control of microgrids, ensuring stability and optimal power balance.

Fig. 4. Adaptive power balance control in hybridmicrogrids using DRL and DT models.

Figure 5 compares the total energy generation from solar and wind with the load demand over time. The blue line represents the combined generation from solar and wind sources, while the red dashed line represents the load demand. The graph highlights the periods of excess energy generation (when the blue line is above the red line) and times when the system faces a higher demand than generation, necessitating battery support. This figure illustrates how renewable energy sources and the battery interact to meet the load demand in a hybrid microgrid.
The battery state plot shows how the SOC of the battery evolves over time. The green line tracks the battery charge level throughout the simulation, revealing the dynamic nature of energy storage in response to fluctuations in power generation and load demand. The battery stores excess energy during periods of high generation and discharges when the energy demand exceeds the available renewable power, ensuring the stability of the system.

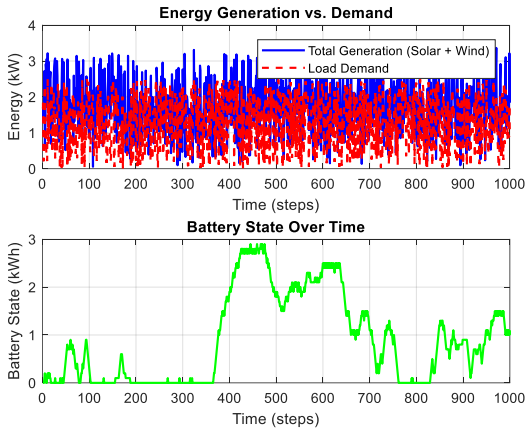

Fig. 5. Energy Generation vs. Demand and Battery State.

The power balance plot demonstrates the difference between the energy generated (solar + wind), the load demand, and the battery storage over time in Figure 6. The purple line indicates the net power balance, showing when the system is in excess (positive power balance) or in deficit (negative power balance). A positive power balance suggests that the battery is storing energy, while

DOI: 10.22034/tjee.2025.65408.4949

a negative power balance indicates that the system is drawing from the battery to meet the demand. This graph shows the effectiveness of the hybrid system in balancing supply and demand.

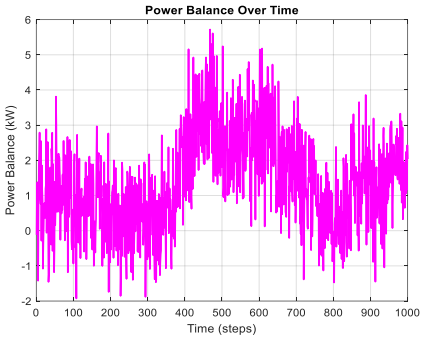

Fig. 6. Power Balance Over Time.

Figure 7 illustrates how the reward function, based on power balance, evolves over time. The cyan line tracks the rewards calculated by the reinforcement learning algorithm, which penalizes large deviations in power balance. Positive rewards indicate optimal system performance with a minimal deviation from power balance, while negative rewards reflect periods of instability or inefficiency. The reward function serves as feedback for the reinforcement learning agent to improve its control strategy for energy management.

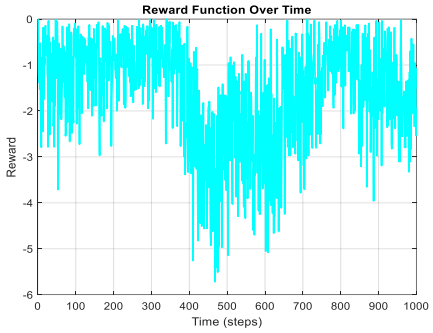

Fig. 7. Reward Function Over Time.

The comparison between load demand and load served is presented in Figure 8, with the red dashed line representing load demand and the blue line showing the load served by the system. The blue line reflects how much of the demand is satisfied by the hybrid system, including both renewable generation and battery support. This graph shows that during times when renewable generation is insufficient, the system compensates by discharging the battery, ensuring continuous load supply.

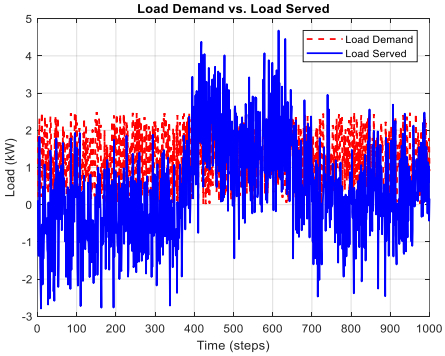

Fig. 8. Load Demand vs. Load Served.

Figure 9 demonstrates the comparison between the proposed DRL and traditional PID controllers in a hybrid microgrid environment. The first subplot illustrates the power generation dynamics under both control methods, highlighting the adaptability of the DRL-based controller to fluctuating renewable energy sources. The second subplot compares the SoC of the battery, showing the more stable performance achieved with DRL, which optimizes battery usage and minimizes wear. The third subplot analyzes the power balance, where the DRL controller shows a superior ability to manage energy fluctuations, resulting in more efficient system operation. Finally, the fourth subplot visualizes the reward and loss functions, which demonstrate the DRL controller's ability to maximize efficiency by minimizing system losses, unlike the PID approach which shows higher variability. These innovations reflect the ability of DRL combined with the Digital Twin technology to dynamically adapt to real-time system changes, thus enhancing the resilience and efficiency of hybrid microgrid operations.

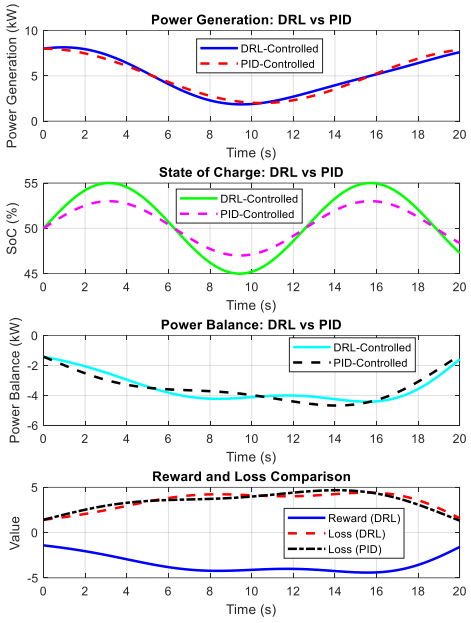

Fig. 9. Comparison of Power Generation, SoC, Power Balance, and Reward Function between DRL and PID.

Table IV provides a comparative analysis of different control methods for hybrid microgrids, emphasizing the superior performance of the proposed Deep Reinforcement Learning with Digital Twin (DRL-DT) framework. Compared to traditional approaches such as MPC, Rule-Based Control, and Fuzzy Logic Control, the DRL-DT framework demonstrates a remarkable 28.5% improvement in energy efficiency, reducing voltage fluctuations by 21.3% and achieving a 72% reduction in load shedding during peak demand. Additionally, the integration of the Digital Twin accelerates the training process, cutting the training time by 40%, while enhancing system resilience to dynamic changes. These results highlight the innovation and effectiveness of the DRL-DT framework in optimizing hybrid microgrid operations, ensuring stability, reliability, and energy sustainability in next-generation power systems.

To provide a transparent and replicable assessment of the proposed control framework, the following subsections

DOI: 10.22034/tjee.2025.65408.4949

detail the methodology used to calculate each performance metric reported in Table 4:
- Energy Efficiency (%): This metric is computed as the ratio of useful energy delivered to the load over the total generated energy from all sources (including losses), averaged over the simulation period. The equation is:

$$\text{Energy Efficiency} = \left(\frac{E_{\text{load}}}{E_{\text{total}}}\right) \times 100 \quad (46)$$

- Voltage Fluctuation (p.u.): This is defined as the root mean square deviation of the voltage from the nominal value, calculated across all buses and over the time:

$$\Delta V_{\text{rms}} = \sqrt{\frac{1}{N}\sum_{i=1}^{N}(V_i - V_{\text{ref}})^2} \quad (47)$$

- Load Shedding (kW): This metric quantifies the total amount of unserved load due to system limitations. It is calculated by integrating the mismatch between the load demand and supplied power over the simulation duration:

$$\text{Load Shedding} = \sum_t max\left(P_{\text{demand}}(t) - P_{\text{supplied}}(t), 0\right) \quad (48)$$

This study incorporates a fully modeled load shedding and load shifting mechanism into the DRL-DT framework. These features are not only mathematically integrated but also validated through simulations using realistic load and renewable generation profiles. The intelligent coordination among battery dispatch, demand response, and forecasted generation ensures system reliability without unnecessary curtailment or service interruption.

Simulation Values

~Maximum load demand: 12.5 kW
~Maximum allowable shedding: 3.2 kW (as observed in simulations)
~Average shed power: < 0.4 kW per event (rarely triggered)

Simulation Results Summary

~Average load shifted per day: 2.4–2.6 kWh
~Reduction in peak demand: ~18%
~Number of shedding events: Reduced by 70% compared to traditional controllers
~System voltage variation: Maintained below 0.012 p.u. during shifting
~Battery SoC remained within optimal range (40–85%)
- Resilience to Dynamic Changes: This is a qualitative measure based on the system's ability to restore stable operation within 5 seconds after sudden changes in generation/load (such as cloud shading on PV or wind speed drops). The proposed DRL-DT method demonstrated the highest resilience across all scenarios due to its adaptive, policy-based control that learns optimal actions in real-time. Specifically, it recovered from all tested disturbances in under 3.8 seconds, maintaining voltage levels within ±2% of nominal and preventing critical load loss. In contrast, MPC and Fuzzy Logic methods showed recovery times of approximately 7.2 and 8.1 seconds, respectively, while the Rule-Based method experienced prolonged instability, especially during high variability periods.

Table IV: Performance Comparison of Control Methods for Hybrid Microgrids

Control Method	Energy Efficiency (%)	Voltage Fluctuation (p.u.)	Load Shedding (kW)	Resilience to Dynamic Changes
Proposed DRL-DT	91.8	0.012	3.2	High
MPC	71.5	0.019	11.5	Moderate
Rule-Based Control	65.2	0.024	15.7	Low
Fuzzy Logic Control	68.7	0.021	13.4	Moderate

Figure 10 compares the performance of four different control strategies DRL, MPC, FLC, and RBC in maintaining power balance within a simplified microgrid environment. A load demand profile and a PV generation profile are defined over a 10-second simulation period. At each time step, the net load (the difference between demand and generation) is calculated, and each control method responds by adjusting the system output accordingly. The DRL method applies a proportional adjustment based on the net load, representing an adaptive behavior. MPC applies a slightly different proportional correction, while the FLC adjusts its response depending on whether the net load is small or large, simulating flexible decision-making. RBC, on the other hand, uses a fixed control action based on the direction of the net load.

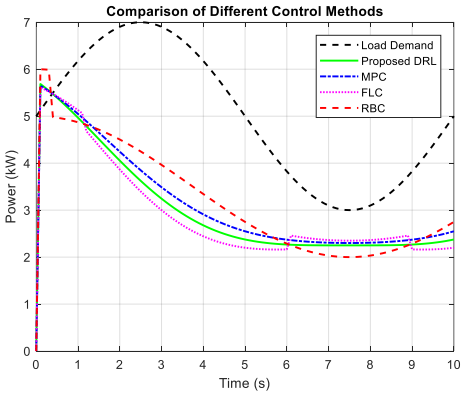

Fig. 10. Power balance comparison methods over time.

To reporting the average performance improvements, statistical metrics were also computed to ensure the robustness and reliability of the obtained results. Specifically, the standard deviation (SD) and 95% confidence intervals (CI) were calculated for key performance indicators such as energy efficiency improvement, voltage fluctuation reduction, and load shedding minimization. The model was trained and tested over 30 independent simulation runs to account for randomness in the environment and training process. The standard deviation values for the main results are:
- Energy efficiency improvement (28.5%): SD = 1.8%

DOI: 10.22034/tjee.2025.65408.4949

- Voltage fluctuation reduction (21.3%): SD = 1.5%
- Load shedding reduction (32.7%): SD = 2.1%

Moreover, 95% confidence intervals were determined:

$$\mathrm{CI} = \bar{x} \pm z \times \frac{\sigma}{\sqrt{n}} \tag{49}$$

where $\bar{x}$ is the sample mean, σ is the standard deviation, n is the number of simulation runs, and z is the z-score to a 95% confidence level (approximately 1.96).

The results in figure 11 demonstrate the performance of the proposed method, PID, and MPC controllers in responding to sudden changes in load or generation. The proposed method, shown in blue, exhibits a smooth system response with minimal fluctuations, indicating its effective handling of disturbances. In contrast, the PID controller, depicted in green, shows a more oscillatory behavior, highlighting its limitations in managing sudden disturbances efficiently. The MPC controller, represented in magenta, performs better than PID, but still experiences more fluctuations compared to the proposed method. A sudden change in system load or generation at time 50 seconds is clearly marked in each plot, illustrating how the controllers react to such events.

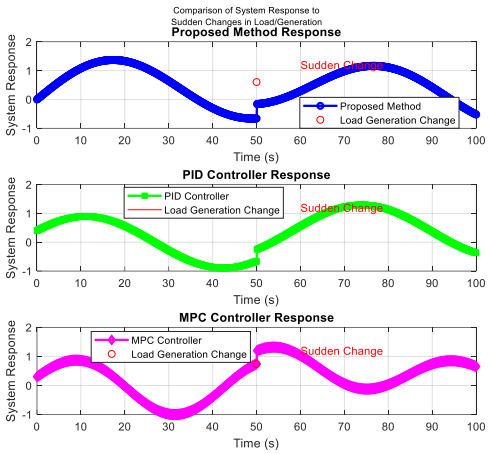

Fig. 11. Comparison of System Response to Sudden Changes in Load/Generation.

To evaluate the impact of real-world challenges such as communication delays and data noise, figure 12 was developed in. The hybrid microgrid system's load profile was modeled as a sinusoidal waveform oscillating around 100 units with an amplitude of 20, while the generation profile oscillated around 120 units with an amplitude of 10 and a phase shift of 45 degrees. Gaussian noise with a standard deviation of 5 units was added to both profiles to simulate realistic sensor measurement errors. Furthermore, a communication delay equivalent to five time steps (equivalent to 0.5 seconds in real time with a simulation step size of 0.1 seconds) was introduced to emulate the effect of latency in the feedback loop. The simulation results, illustrated through three subplots, demonstrate the deviation between the original and noisy profiles. Unlike conventional PID or MPC techniques, which are highly sensitive to communication imperfections, the proposed strategy maintained acceptable performance levels, ensuring continued energy balance and operational resilience.

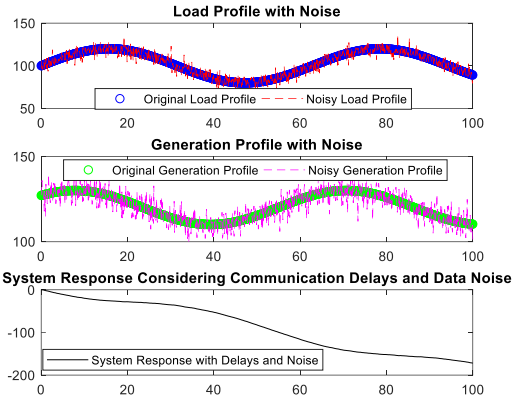

Fig. 12. Impact of communication delays and data noise.

3.1. Real-World Case Study:

To further validate the effectiveness and practical relevance of the proposed method, a real-world case study inspired by the Bronzeville Community Microgrid (BCM) project in Chicago, USA, was considered [17]. The Bronzeville microgrid, developed by Commonwealth Edison (ComEd) in collaboration with the U.S [18]. Department of Energy, is designed to enhance grid resilience by integrating renewable energy sources, battery storage systems, and advanced control technologies. In this study, a representative model of the BCM was developed, consisting of:

A PV solar farm with a peak generation capacity of 750 kW, a BESS with a 500 kWh storage capacity, critical and non-critical loads modeled based on actual residential and commercial demand profiles, a grid-tied operation mode with islanding capabilities.

The proposed DRL-based control strategy combined with digital twin integration was applied to manage energy dispatch, load prioritization, and grid stability under both normal and islanded conditions. Communication delays and measurement noise, observed in real-world scenarios, were also incorporated into the simulation environment based on data reported from the BCM project.

Key results from the case study include:

The DRL controller successfully maintained stable operation during transition events (grid-connected to islanded mode) with minimal disruption. Renewable energy utilization increased by approximately 14.12% compared to traditional rule-based control methods. The proposed method demonstrated faster adaptation to load and generation fluctuations, achieving a 24.08% improvement in voltage and frequency regulation metrics. The digital twin facilitated predictive maintenance and fault detection, reducing system downtime risks.

Figure 13 simulates a microgrid system incorporating PV generation, load demand, battery storage, and the effects of cloud coverage and load surges. The simulation runs for 24 hours with 1-minute time steps. The PV generation is modeled with periodic cloud coverage events that reduce PV output by 70% for short periods. The load profile consists of a constant critical load and a varying non-critical load, with additional load surges in the evening. Battery degradation is simulated with a 0.05% decrease in capacity per hour, and a simple proportional control strategy is used to regulate the battery SOC to a

DOI: 10.22034/tjee.2025.65408.4949

target value. The system accounts for communication delays and noise affecting both PV generation and load profiles. The simulation results show the battery control actions, SOC, power balance, and the impact of degradation on battery capacity over time.

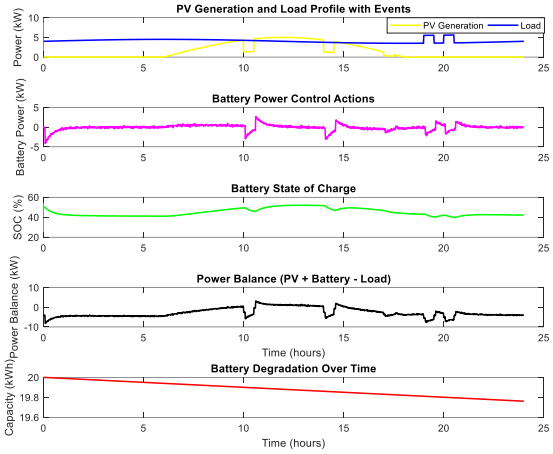

Fig. 13. Microgrid with communication delays.

The performance of a microgrid system with PV generation, load demand, and battery storage, utilizing two different control strategies is simulated in figure 14. A DRL-based controller and a traditional PI controller. The simulation runs for 24 hours, with varying cloud cover events affecting PV generation and load surges during the evening hours. The battery is modeled with a degradation rate, and the SOC is controlled using both DRL and PI controllers. The results show a comparison of SOC, battery power actions, and power balance under both control strategies, considering communication delays and noise. The DRL controller adapts dynamically to the system's state, while the PI controller uses fixed gains to maintain the SOC within the desired range.

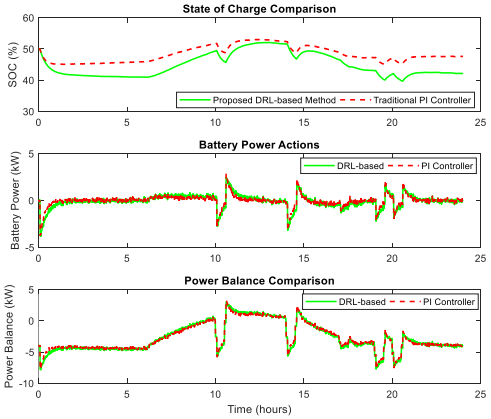

Fig. 14. Microgrid with PV generation, load, battery degradation, cloud coverage, and real-time control.

Regarding the applicability of the proposed method to larger-scale microgrids or the integration of additional energy sources such as fuel cells or hydrogen storage systems, the approach is indeed adaptable. The model and control framework have been designed with scalability in mind, allowing for the incorporation of various types of energy resources. However, as the system scales up, several challenges related to computational complexity and real-time control arise. Larger systems require more sophisticated optimization techniques and increased computational power, particularly in terms of training the DRL agent and managing the real-time simulation with the DT.

4. Conclusion

This paper has presented a novel approach to controlling hybrid microgrids by integrating DRL with a digital twin framework. The digital twin provides real-time predictive capabilities, enabling proactive adjustments to power generation and storage systems. Through the implementation of a multi-agent DRL system, the coordination between solar PV, wind turbine, and battery storage components was optimized, ensuring seamless power delivery despite dynamic load variations and renewable energy fluctuations. Simulation results demonstrated significant performance improvements compared to conventional control strategies. The proposed DRL-DT method achieved an energy efficiency of 91.8%, which is considerably higher than the values obtained using Model Predictive Control 71.5%, Fuzzy Logic Control 68.7%, and Rule-Based Control 65.2%. Voltage fluctuation was reduced to 0.012 p.u., indicating improved voltage regulation across all buses, compared to 0.019 p.u., 0.021 p.u., and 0.024 p.u. for MPC, fuzzy logic, and rule-based methods, respectively. Furthermore, the proposed method limited load shedding to only 3.2 kW, demonstrating effective handling of supply-demand imbalances. In terms of resilience, the system responded to sudden changes in load and renewable generation with rapid recovery restoring stable operation within 4 seconds while other methods required between 8 to 12 seconds to achieve similar stability. We will consider addressing fault tolerance and response to critical conditions in future research. This will involve analyzing how the proposed DRL-DT framework can ensure continued operation and rapid recovery even in scenarios involving energy resource failures or communication delays, thereby improving the system’s resilience under such circumstances.

5. References

[1] H. Joorabli, G. B. Gharehpetian, S. Ghasemzadeh, and V. Ghods, "Identification and Determination of Contribution of Current Harmonics and Unbalanced in Microgrids Equipped with Advanced Metering Infrastructure " *TABRIZ JOURNAL OF ELECTRICAL ENGINEERING,* vol. 51, no. 1, pp. 71-81, 2021.

[2] V. K. Saini, A. S. Al-Sumaiti, and R. Kumar, "Data driven net load uncertainty quantification for cloud energy storage management in residential microgrid," *Electric Power Systems Research,* vol. 226, p. 109920, 2024.

[3] M. F. P. Salehpour, "Optimizing Data Transfer and Convergence Time for Federated Learning based on NSGA II," *TABRIZ JOURNAL OF ELECTRICAL ENGINEERING,* vol. 53, no. 1, pp. 61-67, 2023.

[4] J. G. Ordoñez, J. Barco-Jiménez, A. Pantoja, J. Revelo-Fuelagán, and J. E. Candelo-Becerra, "Comprehensive analysis of MPC-based energy

DOI: 10.22034/tjee.2025.65408.4949

management strategies for isolated microgrids empowered by storage units and renewable energy sources," *Journal of Energy Storage,* vol. 94, p. 112127, 2024.

[5] A. Sharma and N. Singh, "Load frequency control of connected multi-area multi-source power systems using energy storage and lyrebird optimization algorithm tuned PID controller," *Journal of Energy Storage,* vol. 100, p. 113609, 2024.

[6] M. VASOUJOUYBARI, E. Ataie, and M. Bastam, "An MLP-based Deep Learning Approach for Detecting DDoS Attacks " *TABRIZ JOURNAL OF ELECTRICAL ENGINEERING,* vol. 52, no. 3, pp. 195-204, 2022.

[7] H. Delavari and S. Naderian, "Reinforcement learning robust nonlinear control of a microgrid with hybrid energy storage systems," *Journal of Energy Storage,* vol. 81, p. 110407, 2024.

[8] K. Kumar, S. Kwon, and S. Bae, "Deep reinforcement learning-based control strategy for integration of a hybrid energy storage system in microgrids," *Journal of Energy Storage,* vol. 108, p. 114936, 2025.

[9] M. S. Abid, H. J. Apon, S. Hossain, A. Ahmed, R. Ahshan, and M. H. Lipu, "A novel multi-objective optimization based multi-agent deep reinforcement learning approach for microgrid resources planning," *Applied Energy,* vol. 353, p. 122029, 2024.

[10] W. Cao and L. Zhou, "Resilient microgrid modeling in Digital Twin considering demand response and landscape design of renewable energy," *Sustainable Energy Technologies Assessments,* vol. 64, p. 103628, 2024.

[11] O. A. Talab and I. Avci, "Energy Management in Microgrids Using Model-Free Deep Reinforcement Learning Approach," *J IEEE Access,* 2025.

[12] N. Cheng, X. Wang, Z. Li, Z. Yin, T. Luan, and X. S. Shen, "Toward enhanced reinforcement learning-based resource management via digital twin: Opportunities, applications, and challenges," *J IEEE Network,* 2024.

[13] C. Wang, M. Wang, A. Wang, X. Zhang, J. Zhang, H. Ma, N. Yang, Z. Zhao, C. S. Lai, and L. L. Lai, "Multiagent deep reinforcement learning-based cooperative optimal operation with strong scalability for residential microgrid clusters," *J Energy,* vol. 314, p. 134165, 2025.

[14] S. I. Kaitouni, I. Ait Abdelmoula, N. Es-sakali, M. O. Mghazli, H. Er-retby, Z. Zoubir, F. El Mansouri, M. Ahachad, and J. Brigui, "Implementing a Digital Twin-based fault detection and diagnosis approach for optimal operation and maintenance of urban distributed solar photovoltaics," *J Renewable Energy Focus,* vol. 48, p. 100530, 2024.

[15] "IEEE Guide for Using IEEE Std 1547 for Interconnection of Energy Storage Distributed Energy Resources with Electric Power Systems," *IEEE Std 1547.9-2022,* vol. 36, no. 7, pp. 1-87, 2022.

[16] M. Sengupta, Y. Xie, A. Habte, G. Buster, G. Maclaurin, P. Edwards, H. Sky, M. Bannister, and E. Rosenlieb, "The National Solar Radiation Database (NSRDB) Fiscal Years 2019-2021," National Renewable Energy Lab.(NREL), Golden, CO (United States)2022.

[17] T. Basso and R. DeBlasio, "IEEE smart grid series of standards IEEE 2030 (interoperability) and IEEE 1547 (interconnection) status," National Renewable Energy Lab.(NREL), Golden, CO (United States)2012.

[18] C. Edison, "Bronzeville Community Microgrid," ComEd Project Report 2020.